Distribution Agreement

In presenting this thesis or dissertation as a partial fulfillment of the requirements for an advanced degree from Emory University, I hereby grant to Emory University and its agents the non-exclusive license to archive, make accessible, and display my thesis or dissertation in whole or in part in all forms of media, now or hereafter known, including display on the world wide web. I understand that I may select some access restrictions as part of the online submission of this thesis or dissertation. I retain all ownership rights to the copyright of the thesis or dissertation. I also retain the right to use in future works (such as articles or books) all or part of this thesis or dissertation.

 Signature:

_____ _____

Kristen E. Sanders   **Date**

The role of neuronal activity in sensory axon regeneration following sciatic nerve transection and repair in mice.

Author: Kristen E. Weiss Sanders
B.S., Binghamton University, 2010

Graduate Division of Biological and Biomedical Science

Neuroscience

_____

Dr. Arthur W. English
Advisor

_____

Dr. Shannon Gourley
Committee Member

_____

Dr. Shawn Hochman
Committee Member

Accepted:

_____

Lisa A. Tedesco, Ph.D.
Dean of the James T. Laney School of Graduate Studies

_____

Date

The role of neuronal activity in sensory axon regeneration following sciatic nerve transection and repair in mice.

Author: Kristen E. Weiss Sanders

B.S., Binghamton University, 2010

Advisor: Dr. Arthur W. English

An Abstract of a Thesis

Submitted to the Faculty of the James T. Laney

School of Graduate Studies of Emory University

In partial fulfillment of the requirements

For the degree of Master of Science in Neuroscience

Graduate Division of Biological and Biomedical Sciences

Neuroscience

2016

Abstract

The role of neuronal activity in sensory axon regeneration following sciatic nerve transection and repair in mice.

Author: Kristen E. Weiss Sanders

Peripheral nerve injuries (PNIs) are common, and although spontaneous, axon regeneration is slow and inefficient. Increasing activity in injured neurons via exercise has been proposed to drive neuronal BDNF expression, required for enhanced axon regeneration (Gomez-Pinilla et al., 2001; Wilhelm et al., 2012). I attempted to support this hypothesis through inhibition of neuronal activity with an inhibitory DREADD (Designer Receptor Exclusively Activated by Designer Drug). Once I was unable to achieve DREADD expression in sciatic motoneurons following intramuscular injections of AAV-DREADD vectors, I turned to an optogenetic approach to study sensory neurons, often ignored in PNI literature. I first characterized the proportion of sciatic dorsal root ganglion neurons (DRGs) which expressed YFP in an Advillin-Cre::YFP^f reporter mouse. YFP+ visualizes expression of Cre-recombinase under the regulatory element *Advillin*, a sensory-neuron specific gene highly expressed in PNS ganglia (Zurborg et al., 2011). I found that a low percentage of sciatic DRGs (L4: 8.57% ± 1.92%; L5: 7.71% ± 2.35%) expressed YFP (were Cre+). However, Cre+ cells were biased towards larger sciatic DRGs in this strain. When exercised, the lengths of regenerating axons of the sensory neurons in Advillin-Cre::YFP^f mice was increased in a manner similar to what has been observed in all (sensory and motor) axons after exercise. However, whether the activity of axotomized sensory neurons increases during exercise remains unknown. Additionally, factors other than activity could explain any enhancement of sensory axon regeneration with exercise. Repeating experimental results reported here will be an important first step in formulating further testable hypotheses.

The role of neuronal activity in sensory axon regeneration following sciatic nerve transection and repair in mice.

Author: Kristen E. Weiss Sanders

B.S., Binghamton University, 2010

Advisor: Dr. Arthur W. English

A Thesis submitted to the Faculty of the James T. Laney

School of Graduate Studies of Emory University

In partial fulfillment of the requirements

For the degree of Master of Science in Neuroscience

Graduate Division of Biological and Biomedical Sciences

Neuroscience

2016

Acknowledgments

Table of Contents

Introduction

Peripheral nerve injury (PNI) is common, with nearly 3% of trauma patients having damage to one or more peripheral nerves (Noble et al., 1998). Currently, nerve transections are repaired surgically, suturing together the two cut ends. Considerable advances in associated surgical technique have been made over the last 30 years; however, functional outcomes remain poor, with only 10% of adult patients ever recovering full movement of the injured limb (Scholz et al., 2009). For the rest- hundreds of thousands of Americans each year- damage to peripheral axons leaves them permanently debilitated. Experimentally, facilitating axon regeneration in the injured limb, either by a single application of electrical stimulation to the injured nerve (Gordon et al., 2009) or by exercise during recovery from a nerve transection (Sabatier et al., 2008) results in improved functional recovery. Application of exercise as a therapy for PNI in human patients is an attractive option; however, it is essential to understand the underlying cellular mechanisms and requirements for exercise-enhanced axon regeneration before it can be effectively applied to the wide variety of peripheral nerve injuries seen clinically.

Increased activity in injured neurons via exercise has been proposed to drive neuronal BDNF expression, which is required for enhanced axon regeneration (Gomez-Pinilla et al., 2001; Wilhelm et al., 2012). However, this hypothesis has not been tested, and other aspects of exercise could contribute significantly. While exercise is a promising and highly translatable therapy potential for peripheral nerve injury, its underlying mechanisms and effects on functional recovery are not yet sufficiently understood to foster that translation. By experimentally isolating and manipulating activity of injured neurons, we can examine the necessity for neural activity in promoting axon regeneration without the presence of additional confounding exercise-related variables.

I attempted to investigate the role that activity plays in regenerating axons through the inhibition of sensory neuron activity following sciatic nerve transection and repair. My first approach was to explore this question pharmacogenetically via the application of Designer Receptors Activated Exclusively by Designer Drugs (DREADDs) (Nichols and Roth, 2009) coupled with a custom adeno-associated viral (AAV)-9 vector carrying the genes for the hM4Di construct (an inhibitory DREADD) under the neuron-specific human synapsin promoter (AAV9-hSyn-hM4Di-mCherry). When my attempts to express hM4Di at physiologically relevant levels in our target neuronal population were unsuccessful, I moved to an optogenetic approach to investigate similar proposed questions.

As our investigations regarding the role and requirement of active neurons in regenerating nerves continue, it has become clear that it is very important to the overall picture to ask these questions separately in motor and sensory neuron populations. Much of the work in PNI literature has focused solely on MNs, despite great recent developments in neuronal subtype-specific techniques. It is unknown if it is MN activity, sensory neuron activity, or both that could be key to axon elongation following PNI, and if activity in either of these neuronal subtypes effects axon elongation of the other. Therefore, the optogenetics portion of my project concentrated on characterization of YFP expression in the Advillin-Cre::YFP[f] reporter mouse. Advillin-Cre transgenic mice express Cre-recombinase under the regulatory element *Advillin* (Adv), is a sensory-neuron specific gene expressed at high levels in PNS ganglia (Zurborg et al., 2011). ***The overall goal of this thesis has been to evaluate the role of sensory neuron activity in regeneration of afferent following peripheral nerve injury.***

Chapter I:
Attempted use of AAV9-hm4Di vectors to target spinal motoneurons

Introduction

Initially, our attempts to experimentally explore the role of neuronal activity in axon regeneration following peripheral nerve injury (PNI) were largely driven by the collective application of two emerging and advancing technologies in biomedical research:

First, the use of **Designer Receptors Activated Exclusively by Designer Drugs (DREADDs)** (Nichols and Roth, 2009) allows for specific, non-invasive alteration of neuronal activity in awake, behaving animals while leaving other physiological variables that might be related to exercise unchanged. Experiments were designed to utilize the hM4Di DREADD, a Gi-coupled GPCR engineered from the M4-muscarinic receptor (Armbruster et al., 2007). This DREADD can be activated acutely or chronically with its ligand, clozapine-N-oxide (CNO) to inhibit neuronal firing. Previously, cortical, basal ganglia, and midbrain pathways had been investigated via localized expression of a DREADD in various neuronal populations (Farrell and Roth, 2013). I attempted to extend the experimental potential of this technology through the use of DREADDs expressed in neurons whose axons are found in peripheral nerves.

Second, a custom **adeno-associated viral (AAV)-9 vector** carrying the genes for the hM4Di construct under the neuron-specific human synapsin promoter (AAV9-hSyn-hM4Di-mCherry) was used to target DREADD expression to the L3-5 motor neuron pool. Extended use of DREADD technology to alter neuronal activity in the periphery has not yet been analyzed. While multiple routes of administration have been attempted to achieve MN and/or sensory neuron transduction with AAV-based vectors, I used a series of intramuscular injections into mouse hind limb muscles and evaluated hM4Di expression visually via fluorescence microscopy at various time points following injection

(Table 1). I hypothesized that this approach would result in infection of L3-5 MNs with AAV9, therefore resulting in expression of the hM4Di DREADD in only these cells, making the use of inhibitory DREADD technology in MNs of behaving mice possible without creating lethal suppression of all MN function.

My hope was that this innovative combination of AAV vector technology with DREADD constructs could allow elegant isolation of targeted cells for the manipulation of neural activity.

Material and Methods

AAV-based viral vector injection. All procedures were approved by the Institutional Animal Care and Use Committee of Emory University and conformed to the Guidelines for the Use of Animals in Research of the Society for Neuroscience. All mice used were maintained on a C57BL/6J background, and were backcrossed for at least six generations. Ten wild type (WT) mice were injected with an AAV8-hSyn-hM4Di vector and two more were injected with an AAV9-CMV-hM4Di vector. All AAV-based viral vectors were injected through the shaved skin into one or more mouse calf muscles. Multiple small volume intramuscular injections were given in an attempt to minimize damage to muscle and maximize neuronal exposure to the vector. The total volume injected in each mouse is shown in Table 1. The axons of motoneurons (MNs) in L3-5 spinal cord contribute to the sciatic nerve and innervate tibialis anterior (TA), a hind limb flexor, and gastrocnemius (GAST), a hind limb extensor (English, 2005). Injection of one or more of these muscles in each animal allowed me to target L3-5 MNs to provide a basis for later work using the sciatic nerve transection and repair model that has been extensively used for previous studies the English lab.

The AAV8-hSyn-hM4Di and AAV9-CMV-hM4Di vectors with these specific serotype and promoter combinations were readily available for purchase from the Vector

Core at the University of North Carolina at Chapel Hill (UNC Vector Core). The human synapsin (hSyn) and cytomegalovirus (CMV) promoters have both been shown to produce selective neuronal transduction in rodents (Kugler et al., 2003; van den Pol and Ghosh, 1998). While the titer of viruses purchased from the UNC Vector Core can vary, they are guaranteed to be at least 1 x 10^{12} vp/mL (viral particles per mL) of viral vector. There are multiple examples in the literature that demonstrate this titer (or even less) to be adequate for significant neuronal transduction (Benkhelifa-Ziyyat et al., 2013; Duque et al., 2009; Federici et al., 2012; Fortun et al., 2009; Kaspar et al., 2003; Rahim et al., 2011).

AAV9-hSyn-hM4Di-mCherry viral vector construction. We were able to work with our in-house Viral Vector Core of the Emory Neuroscience NINDS Core Facilities to obtain another AAV-based vector. Plasmids encoding a neuron-specific (hSyn) promoter and the hM4Di Gi-coupled DREADD construct (Armbruster et al., 2007) (a generous gift of Dr. Bryan Roth, University of North Carolina, Chapel Hill), and the AAV2/9 packaging system were used to construct the AAV9-hSyn-hM4Di-mCherry vector that was then injected into ten additional mice. The titer of this vector was 2 x 10^{13} vg/mL (viral genomes/mL). This titer was the same as that used in another study utilizing the AAV-based viral vector, in that case in non-human primates (Samaranch et al., 2013).

Analysis of hM4DI-mCitrine and hM4Di-mCherry expression in spinal cord. At a varying number of weeks following AAV9-hM4Di injection (see Table 1), each animal was injected with 0.1% cholera toxin B (CTxB) (Hirakawa et al., 1992) conjugated to Alexafluor 488, a retrograde neuronal marker. In an attempt to back-label the same pool of neurons transduced with the viral vectors, a total of five 0.5 µL injections, two into lateral GAST, two into medial GAST, and one into TA, were administered to each animal. Three days later, animals were anesthetized via intraperitoneal injection of pentobarbital (150 mg/kg) and transcardially perfused with 0.9% saline and 4%

paraformaldehyde. Spinal cord segments corresponding to L3-L5 vertebrae were harvested and used to prepare 20 μm horizontal (AAV8 animals) or transverse (AAV9 animals) cryostat sections which were mounted onto microscope slides using ENTELLAN (Merck KGaA; distributed by EMD Millipore Corporation in the USA). As fluorescence of these proteins can fade in fixed tissue, I used our standard lab protocol to perform immunohistochemistry (IHC) with an rabbit α-GFP (green fluorescent protein; Invitrogen) on the tissue from the animal injected with the AAV9-CMV vector (expressing mCitrine) and with a rabbit α-RFP (red fluorescent protein; Abcam) antibody on the tissue from the animals injected with the AAV9-hSyn vector (expressing mCherry). The specific α-RFP antibody was used and suggested by the Roth lab at UNC Chapel Hill, which pioneered much of the DREADD technology. Work from our colleagues in the Rainnie lab confirmed that visualizing DREADD expression in fixed tissue is difficult, but I was able to effectively use this antibody to confirm mCherry expression with α-RFP in some of their control tissue that had been injected with a similar AAV9 vector. Fluorescence images of these sections from my animals were used to determine the number of transduced neurons (expressing mCitrine or mCherry) out of the total number of MNs innervating TA and GAST (visible by their expression of Alexafluor 488).

Table 1. Intramuscular injection of DREADD-expressing vectors (n=22).

	AGE	VIRUS	MUSCLE	VOLUME	WKS post-AAV
1	adult	AAV8-hSyn	L-TA / R-MG	0.5 µL/ 2 x 0.5 µL	2.5
2	adult	AAV8-hSyn	L-TA / R- MG	0.5 µL/ 2 x 0.5 µL	2.5
3	adult	AAV8-hSyn	L-MG / R-TA	2 x 0.5 µL/ 0.5 µL	2.5
4	adult	AAV8-hSyn	L-MG / R-TA	2 x 0.5 µL/ 0.5 µL	2.5
5	adult	AAV8-hSyn	L-TA	0.5 µL	3
6	adult	AAV8-hSyn	R-MG	2 x 0.5 µL	3
7	adult	AAV8-hSyn	R-TA	0.5 µL	3.5
8	adult	AAV8-hSyn	R-MG	2 x 0.5 µL	3.5
9	adult	AAV8-hSyn	R (LG/MG/TA)	2 x 0.5 µL / 2 x 0.5 µL / 0.5 µL	4
10	adult	AAV8-hSyn	R (LG/MG/TA)	2 x 0.5 µL / 2 x 0.5 µL / 0.5 µL	4
11	adult	AAV9-CMV	R (LG/MG)	0.75 µL / 0.75 µL	4
12	adult	AAV9-CMV	R (LG/MG/TA)	2 x 0.5 µL / 2 x 0.5 µL / 0.5 µL	4
001	adult	AAV9-hSyn	R-MG	4 x 0.5 µL	23.5
002	adult	AAV9-hSyn	R-LG	4 x 0.5 µL	23.5
003	adult	AAV9-hSyn	R (LG/MG/TA)	2 x 0.5 µL / 2 x 0.5 µL / 0.5 µL	15
004	adult	AAV9-hSyn	R (LG/MG/TA)	2 x 0.5 µL / 2 x 0.5 µL / 0.5 µL	8
005	adult	AAV9-hSyn	R (LG/MG/TA)	2 x 0.5 µL / 2 x 0.5 µL / 0.5 µL	15
006	adult	AAV9-hSyn	R (LG/MG/TA)	2 x 0.5 µL / 2 x 0.5 µL / 0.5 µL	15
015	P6	AAV9-hSyn	R-GN	0.1 µL	8
016	P6	AAV9-hSyn	R-GN	0.1 µL	8
019	P6	AAV9-hSyn	R-GN	0.1 µL	14.5
020	P6	AAV9-hSyn	R-GN	0.1 µL	14.5

One of three AAV-based vectors was injected into the specific calf muscles of 22 mice, including tibialis anterior (TA), medial gastrocnemius (MG), and lateral gastrocnemius (LA). Injection of the left (L), right (R), or both legs varied by subject. Animals labeled as "adult" were at least eight weeks of age. These mice then underwent retrograde tracing of sciatic neurons innervating the calf muscles and were euthanized at various time points following viral vector injection. All AAV-based vectors listed here included the hM4Di (inhibitory DREADD) construct attached to a fluorescent protein (mCitrine for AAV8-hSyn and AAV9-CMV; mCherry for AAV9). The titer of the AAV8-hSyn and AAV9-CMV viral vectors (animals 1-12) from the UNC Vector core varies, but is guaranteed to be at least at least 1×10^{12} vp/mL. The titer of the in-house AAV9-hSyn vector is 2×10^{13} vg/mL (animals 001-006, 015-016, and 019-020).

Results and Discussion

Work in the emerging field of "pharmacogentics" has successfully applied DREADD technology to manipulate neuronal activity in the mammalian brain. Over the past several years, work in the English lab has demonstrated that exercise significantly enhances axon regeneration following cut and repair of the mouse sciatic nerve and has led to the hypothesis that activation of injured neurons is required for this effect. As a strategy to investigate this hypothesis, I attempted use AAVs to express DREADDs in the peripheral nervous system, allowing me to alter the activity of injured sciatic motoneurons (MNs) and/or sensory neurons.

Based on a 2010 paper (Fortun et al.) that successfully transduced sciatic MNs following intramuscular injections of AAV vectors, I injected AAV into the calf muscle(s) of 22 mice, varying serotype, promoters, injection volume, age at injection, and time between injection and experimental endpoint (Table 1). My outcome measure for achieving transduction of my target neurons was to examine fixed tissue for the fluorescent DREADD fusion protein (marked by mCitrine for AAV8, mCherry for AAV9). In spinal cord sections prepared from 22 animals, every third section was studied. The tissue of two mice was reacted with antibodies to GFP and the tissue of another ten mice with antibodies to RFP, based on the fluorescent protein expressed by the associated DREADD construct. The ventral horn of the spinal cord was searched for labeled MNs in approximately 21 horizontal or 55 transverse sections per mouse (n=22). I was unable to detect evidence of DREADD transduction in any sciatic MNs.

Injection of viral vectors into the hind limb muscles was considered the optimal route of administration to result in adequate MN transduction of the L3-L5 MN pool (sciatic motoneurons). One option to increase the number of MNs transduced would have been to simply inject more of the viral vector. However, given the small size of the targeted muscles it would have likely been impossible to inject additional virus without

leakage and exposure of non-targeted muscles to the virus. It is also possible that the

time needed for effective retrograde transport and viral transduction of MNs after

injections into the muscles of adult animals might be longer than any of those included in

my series of experiments (Table 1).

Options considered other than increasing viral concentration include using a

different route of viral vector administration. Both intravascular (Foust et al., 2009) and

intrathecal (Federici et al., 2012) administration of AAV9-based viral vectors have been

used to successfully transduce lumbar spinal cord MNs. Use of a self-complementary

AAV9 viral vector has also been shown to increase efficiency of MN transduction (Duque

et al., 2009). All of the vectors I utilized are single-stranded. Another possibility would

have been to inject into the ventral roots, reducing the distance the virus must travel to

the MN cell bodies. While all of these alternative approaches might be effective in

promoting viral transduction in motoneurons, they lack the ability to restrict expression to

desired populations of motoneurons. Similarly, direct injection of AAV9-hSyn-hM4Di-

mCherry into the spinal cord has been utilized to achieve robust transduction of MNs

(Snyder et al., 2011), but as the hSyn promoter targets expression to multiple neuron

types, injection of AAV9 into the spinal cord would likely also result in undesirable

transduction of interneurons.

Using AAV9-YFP vectors, others in our lab have shown modest MN transduction

following IM injection. Using AAV9-Cre vectors in a similar manner, others in the lab

have now shown robust expression of Cre-dependent channelrhodopsin (ChR2) in

motoneurons. It is possible that the hM4Di cargo itself may interfere with retrograde

transport and AAV9-based viral transduction of MNs, and that the AAV9 vectors carrying

different cargoes simply work better to transduce spinal cord MNs after IM injections in

adult mice than the AAV9-hM4Di vector. Mice expressing Cre-dependent DREADDs,

which could be used in conjunction with the AAV9-Cre vector and resolve the issue of

hM4Di expression in the ventral horn, have only just become obtainable. They were not available for my study.

Using the same hind limb IM injection techniques, the English lab has had some recent success with the use of AAV9-hSyn-hM3Dq-mCherry, which expresses an excitatory DREADD. Physiologically relevant increases in motoneuron excitability were found, indicating substantial motoneuron transduction. However, visualization of the hM3Dq-mCherry fusion protein in the ventral horn has remained problematic (Jaiswal and English, 2015). Using similar techniques to this recent work, I attempted to find physiological evidence that hM4Di was being expressed in L3-L5 MNs but was unable to do so. The AAV9-hSyn-hM3Dq was of a lower titer (7.6×10^{12} vg/mL) than the AAV9-hSyn-hM4Di-mCherry vector that I used, further substantiating the idea that my failure to produce significant DREADD expression in sciatic motor neurons could be remedied by the use of a injecting more volume or a higher titer viral vector. Additionally, my failure to find either anatomical or physiologically results with use of the inhibitory Gi DREADD receptor in comparison to some of those seen with the excitatory Gq DREADD receptor could reinforce the notion that it is simply much more difficult to evaluate inhibition of neuronal activity than excitation using our model system.

Chapter II:
Characterization of Advillin-Cre::YFP^f reporter mice

Introduction

Taking all of the factors impeding the use of inhibitory DREADDs in our experimental paradigm, in addition to progress in other techniques in the lab as a whole, I began to explore experimental alternatives to inhibitory DREADDs that I could use to inhibit and study neuronal activity and axon regeneration after PNI. Advillin-Cre transgenic mice express Cre-recombinase under the regulatory elements of *Advillin* (Adv), a sensory-neuron specific gene expressed at high levels in PNS ganglia (Zurborg et al., 2011). Our lab has successfully crossed Advillin-Cre mice with mice expressing yellow fluorescent protein (YFP) in a Cre-dependent manner to create a reporter strain, in which the cell bodies and axons of only sensory neurons are labeled with YFP, and with mice expressing a Cre-dependent ChR2-YFP^f, in which sensory axons express he light-sensitive cation channel, channelrhodopsin and YFP. Both of these Adv-Cre based mice are very useful in that they enable visualization of exclusively sensory neurons in peripheral nerves, enabling anatomical outcome measures of axon regeneration and muscle reinnervation in our experimental PNI paradigms. In the Adv-Cre::ChR2-YFP^f mice, sensory axons can be activated exclusively using blue light. Given the large proportion of peripheral nerves that are of mixed modality, we wanted to investigate the role of sensory neuron activity in anatomical and functional recovery after PNI in mice.

The goal of my study was to characterize the extent and cell-type specificity of Cre expression in Adv-Cre::YFP^f reporter mice, focusing on the dorsal root ganglion (DRG) cells. This work sought to define a population of DRG neurons with axons in the sciatic nerve that express YFP (and Cre recombinase) in the Adv-Cre::YFP^f mouse line, including analysis of these neurons by size. This study would serve as a necessary foundation for future studies in which DRG neurons could be optically activated by blue

light in the analogous Adv-Cre::ChR2-YFP[f] mouse or inhibited by yellow light in an Adv-Cre::eNpHR2.0 mouse (which expresses halorhodopsin, eNpHR2.0, an inhibitory opsin). We have hypothesized that blocking sensory activity during exercise or electrical stimulation of the sciatic nerve will inhibit the promoting effect of neuronal stimulation of axon regeneration after PNI. Liske et al. (2013) demonstrated that optical stimulation of sciatic motor and sensory axons in Thy1::eNpHR2.0 mice can inhibit motor nerve and muscle activity, indicating that neuronal activity can be inhibited peripherally by light.

Material and Methods

Breeding of Advillin-Cre::YFP[f] mice: Advillin-Cre-ER2 mice were obtained (a generous gift for Dr. Fan Wang, Duke University). The mice express Cre recombinase under the control of the *Advillin* promoter. In our colony, Adv-Cre-ER2 mice were bred with Thy1::YFP[f] mice to create the Adv-Cre::YFP[f] mouse. In both strains of Adv-Cre animals, Cre expression driven by the *Advillin* promoter is achieved only after treatment with tamoxifen, a synthetic estrogen.

Tamoxifen treatment: A solution of 10% ethanol and 90% sunflower oil (Sigma-Aldrich) was used to dissolve powdered tamoxifen. The solution is stored at 4°C. Once reaching adulthood, in order to induce Cre expression, mice are orally administered tamoxifen in this formulation (0.75 mg/20 g body weight) for three consecutive days. A second round of tamoxifen administration is given two weeks later. We then waited at least another two weeks before tamoxifen-treated mice are used experimentally This approach has previously been used successful in our laboratory to work with Cre-dependent transgenic strains (Wilhelm et. al, 2012).

Retrograde tracer experiments: Much as described in Part I, two weeks after sciatic nerve transection and repair, cholera toxin B (CTxB) conjugated to Alexafluor 555 was applied bilaterally to cut axons of the sciatic nerve of five mice. Three days later, animals

were euthanized and perfused. Tissue harvesting then consisted of the collection of L3-L5 dorsal root ganglia, which were used to prepare 16 µm transverse cryostat sections which were mounted onto microscope slides using Vectashield® with DAPI (Vector Laboratories).

Fluorescence microscopy: Based on preliminary analysis, the number of retrogradely labeled neurons in the L3 DRG was quite small, so we chose to analyze data only from L4 and L5 DRGs. For the L4 and L5 DRGs of first two cases (6 DRGs out of 16 total DRGs), fluorescent images were obtained from every tissue section. From counts of these cases, we determined that counting cells in every third serial histological section and multiplying the resulting counts by three resulted in an estimate of the total number of labeled cells that predicted the actual count of the total number of cells acceptably. Sampling every third section was used to image the remaining ten ganglia.

Analysis of retrogradely labeled and Cre+ neurons: In 289 fluorescent image fields obtained from these histological sections, DRG neurons that were retrogradely labeled from AF-555 tracer applied to the sciatic nerve were identified by their red fluorescence. Initially, ImageJ software was used to identify all objects in the image that were fluorescing red. Most of the objects identified were retrogradely labeled cells; however, cell fragments and areas of autofluorescence (those without a blue DAPI-stained nucleus) were visually eliminated. For each cell identified, the cross-sectional area and mean red, green, and blue fluorescence intensity was measured. For each image, the green fluorescence intensity of visually identified YFP+ neurons was determined, irrespective of the intensity of fluorescence in other channels. Among the (red) retrogradely labeled neurons, those with a green (YFP) intensity within the visually determined range were considered to be double-labeled.

Statistics: Co-expression of the red retrograde label and YFP expression in DRG neurons (Fig. 2.1: yellow arrows) identified Cre+ sensory neurons whose axons course

in the sciatic nerve. After the number of doubled-labeled (Cre+) cells was determined for each DRG studied, we pooled the cell size (area) measurements for each mouse and constructed frequency histograms. We compared these histograms for all retrogradely labeled (red) neurons and their relative subset of double-labeled neurons (Figure 2.3).

We observed an expected bimodal distribution of cell sizes and established a separation between large and small cells, based on the literature for mouse DRG neurons (Price, 1985). We then calculated the percentage neurons in the large vs. small groups in a case-wise manner among retrogradely labeled (Cre-) and double-labeled (Cre+) cells. We evaluated the significance of differences in these proportions using an unpaired t-test. Overall, we found a slight but significant bias toward large DRG cells among Cre+ retrogradely labeled sciatic DRG neurons.

Results and Discussion

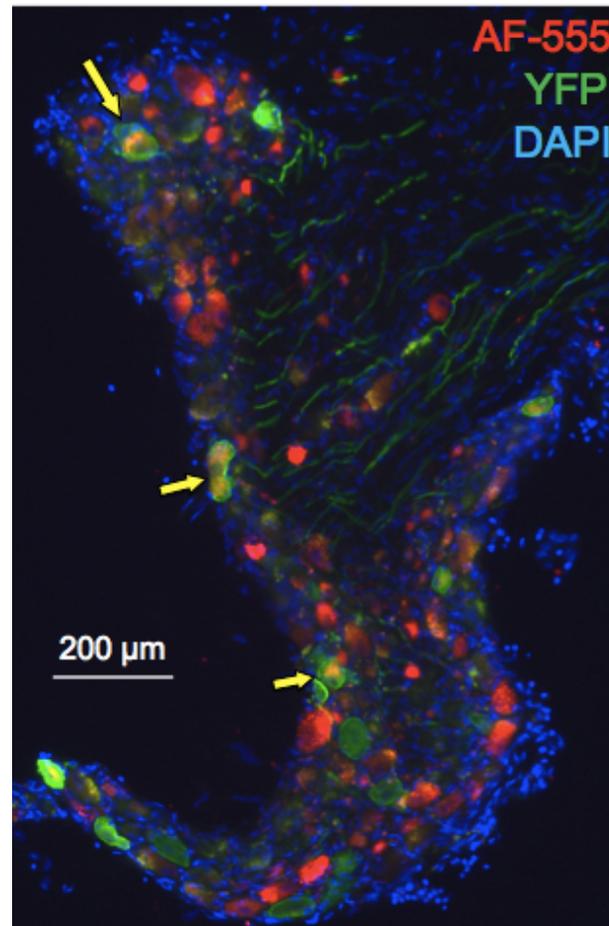*Extent of YFP expression of retrogradely labeled sciatic neurons:* Strong YFP expression was observed in the L4-5 DRG cells of the Advillin-Cre::YFP[f] mouse (Fig 2.1). No YFP expression is observed in the MNs or ventral roots of this transgenic strain (Ward and English, 2015). Only a subset of sciatic DRG neurons in the Adv-Cre::YFP[f] mouse expressed YFP (were Cre+). Only 8.57% ± 1.92% (SEM) of sciatic L4 DRGs and 7.71% ± 2.35% (SEM) of sciatic L5 DRGs also were YFP+ in this transgenic strain (Figure 2.2).

Size distribution of YFP+ (Cre+) retrogradely labeled sciatic neurons: The distributions of the sizes of all retrogradely labeled L4 and L5 DRG cells and the subset of those cells

Figure 2.1. A fluorescent 16 µm section of an L4 DRG from an Advillin-Cre::YFP[f] reporter mouse.
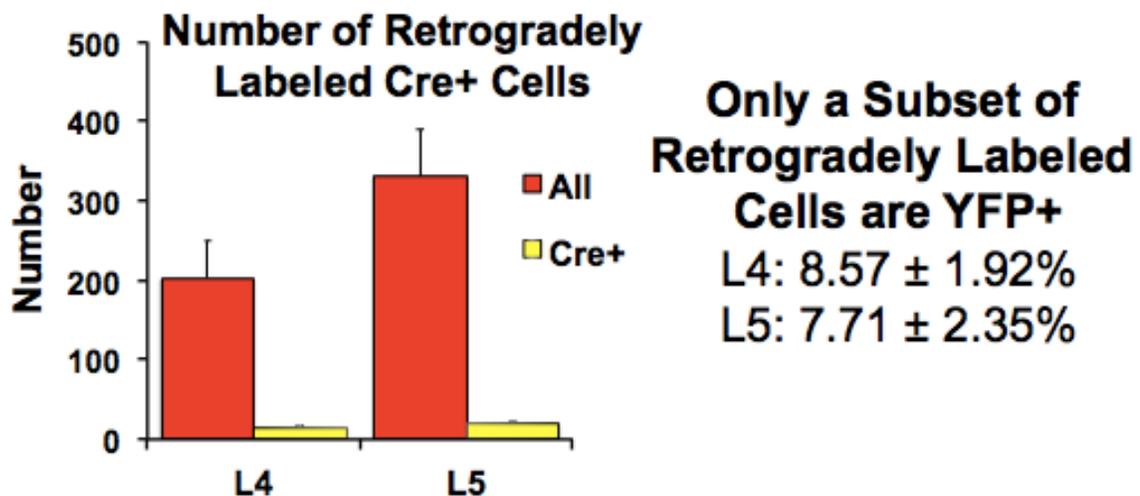

In this image of a section through the L4 DRG of an Advillin-Cre::YFP[f] mouse, DAPI stains the nuclei of all cells blue. Green afferent fibers and cells are YFP+. Red cells are retrogradely labeled with AF-555 dextran crystals following nerve soak. Cells that appear yellow, indicated by the yellow arrows, are double-labeled with YFP and AF-555 are sciatic afferent neurons that are also YFP+.

which were also Cre+ are shown in Figure 2.3. Both size distributions are bimodal, as might be expected for DRG neurons, but the distribution of doubled labeled neurons (Fig. 2.3, yellow bars) is biased slightly toward larger sensory neurons (> 400 µm^2, indicated by the left yellow arrow). Although 30.53% of Cre- DRG neurons are in this large range, significantly more (48.40%) Cre+ DRGs were at least this size (Fig 2.3). We

observed several doubled-labeled cells that were larger (>1100 µm^2, indicated by the right yellow arrow) than any nearly any of the cells that were only retrogradely labeled.
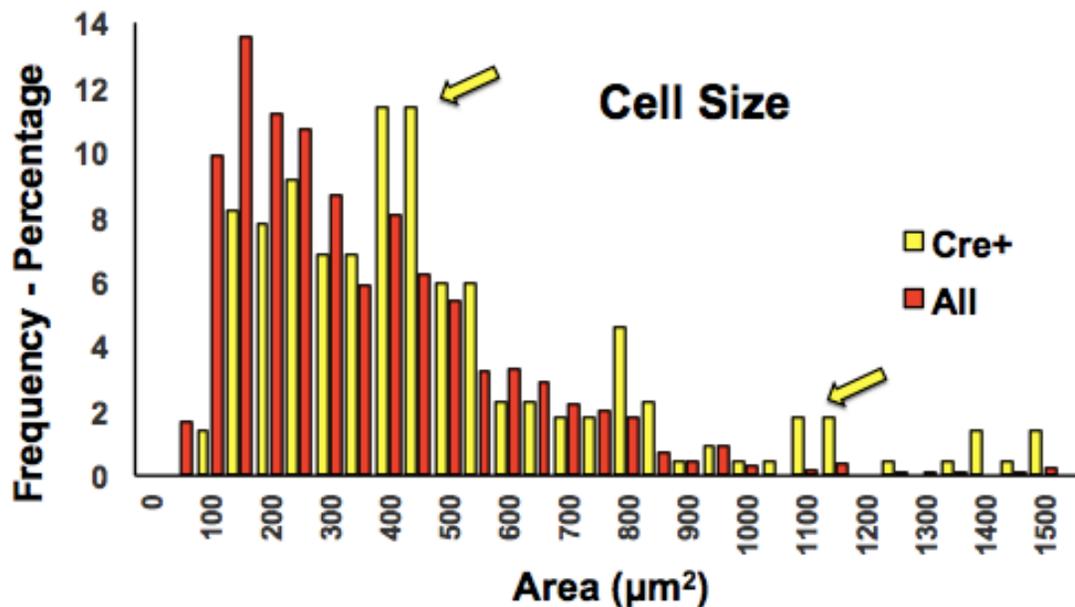
Characterization of the Adv-Cre::YFP^f mouse allowed evaluation of this transgenic animal for future use in our sciatic nerve transection model. Initially, given experience with other transgenic mice in our lab, I expected that the proportion of Cre+ sciatic afferent neurons in this strain would be larger than actually observed and would constitute a representative sample of all sciatic afferent neurons. A relatively small subset DRG neurons with axons in the sciatic nerve in Adv-Cre::YFP^f mice express Cre recombinase. Additionally, this subset is biased slightly, but significantly towards larger cells. Therefore, optical activation in mice such as the Adv-Cre::ChR2-YFP^f mouse will influence a relatively small number of DRG neurons and favor larger cells.

Figure 2.2. Retrogradely labeled L4 and L5 sciatic
DRG cells in Adv-Cre::YFP^f mice (n=5)

Only a relatively small percentage of retrogradely labeled sciatic DRGs in Adv-Cre::YFP^f cells express YFP (Cre+).

Figure 2.3. A size distribution of retrogradely labeled L4 and L5 sciatic DRG neurons in Adv-Cre::YFP^f mice (pooled from n=5 animals)

Cre+ Cells are Biased Towards Larger Sensory Neurons

Cell Type	% Small-Medium (< 400µm^2)	% Large (> 400 µm^2)
All	69.46%	30.53%
YFP+	51.60%	48.40%

A histogram showing the size distribution of all retrogradely labeled (AF-555 positive) and Cre+ (YFP+) DRG cells observed. While the mode in the size of Cre+ cells was at 400 and 450 µm^2 (indicating the left yellow arrow), the distribution of Cre+ cells is positively skewed in comparison to all retrogradely labeled sciatic DRGs. Nearly all retrogradely labeled cells at or above 1100 µm^2 were Cre+.

**Chapter III: The effects of exercise on regeneration of sensory axons
following sciatic nerve transection and repair in mice**

Introduction

Axon regeneration in injured nerves is enhanced by exercise (English et al.,
2014). Earlier observations indicate that increased neural activity associated with
walking drives activity-regulated neuronal BDNF expression required for regeneration
(Gomez-Pinilla et al., 2001), but other aspects of exercise, such as oxygenation state,
environmental enrichment, testosterone stimulation, and caloric utilization also have
been implicated. A recent study has shown that increased neural activity is sufficient to
promote motor axon regeneration after peripheral nerve transection (Ward et al., 2016),
but whether the same is true for regeneration of sensory axons is not known. The
application of treadmill exercise in a PNI and regeneration paradigm has never been
conducted in a setting which allowed the visualization of only sensory fibers following
treadmill training. The use of Adv-Cre::YFP^f mice allowed testing of the hypothesis that
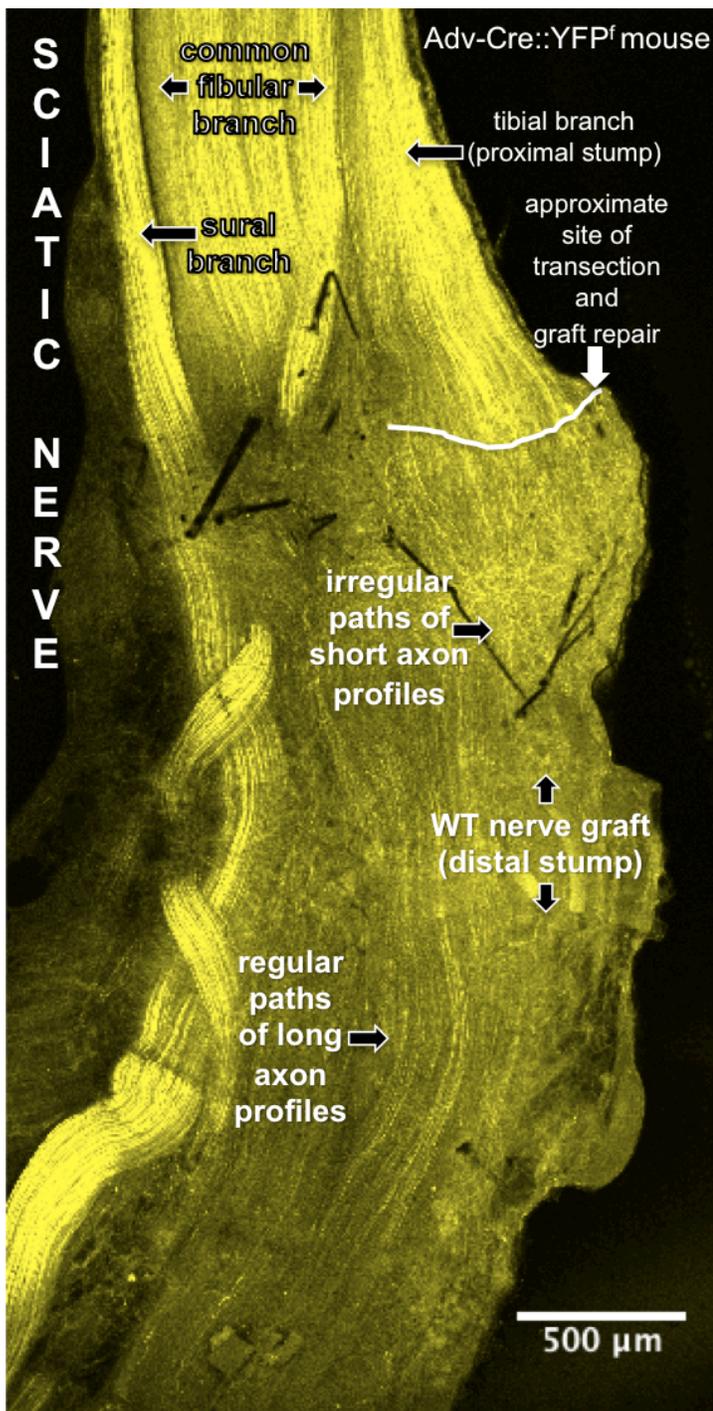exercise enhances sensory regeneration.

Materials and Methods

Nerve transection and graft repair: Eight Adv-Cre::YFP^f mice underwent bilateral
transection and graft repair of the right tibial nerve. The tibial nerve was exposed and
transected approximately 1-2 mm distal to the site at which the sciatic nerve trifurcation
into the common fibular, tibial, and sural nerve occurs. From a strain- and sex-matched
wild-type (WT) donor mouse, a 6-8 mm segment of the tibial nerve was harvested and
used to repair the severed tibial nerve by attaching the proximal end of the WT graft to
the proximal cut segment of the tibial nerve in the host mouse. To prevent the possible
influence of target-derived molecules on regenerating axons, the nerve graft was not
connected to the original distal stump of the cut nerve in the host mouse. To secure the
repair site as a whole and allow the regeneration of fibers into the graft without any

twisting or sliding of the graft, the two nerve ends were placed on a small rectangle of

SILASTIC film (Dow Corning 501-1) and an 8 µl drop of fibrin glue was pipetted onto the

nerve ends (MacGillivray, 2003). This protocol for the repair of peripheral nerves is well

established in the English lab (English, 2005; English et al., 2007).

　　Treadmill training of experimental animals. Three days following tibial nerve

transection and repair, mice began an exercise program. Animals ran on the treadmill in

a sex-appropriate exercise regimen five days a week for two weeks. To promote axon

regeneration in cut nerves, different exercise regimens are required for males and

females (Wood et al., 2012). After the last treadmill training session, mice were

euthanized with phenobarbital and transcardially perfused. Nerves, including grafts,

were harvested, with the location of the cut and repair site identified by the presence of

the SILASTIC mat placed under the nerve stumps during surgery. These mats were

carefully removed from the harvested tissue to avoid damaging the repaired nerve and

then the entire nerve was placed on a microscope slide and cover slipped using

ENTELLAN mounting medium (Merck KGaA; distributed by EMD Millipore Corporation in

the USA).

　　Confocal microscopy and axon profile length analysis. A Leica LSM SP8 confocal

was used to image whole-mounted nerves and obtain stacks of serial optical sections 10

µm thick through the entire depth of the nerve. Corresponding Leica software was used

to stitch sets of images together to reconstruct the repaired nerve and graft in three

dimensions (Fig 3.1). Because no fluorescence is inherent to the grafts from WT mice

used to repair these nerves profiles of regenerating axons from the Adv-Cre::YFP[f] host

mouse which grow past the transection site and into the WT graft were readily visible in

confocal images. ImageJ software was then used to measure the length of all YFP+

axon profiles in the graft. This method has been previously described in detail (English,

2005; Groves et al., 2005).

Figure 3.1. A confocal image of a transected Advillin-Cre: YFP^f tibial nerve with regenerating axons growing into the WT graft.

This image is from a single 10 μm optical section from a nerve in an Adv-Cre::YFP^f mouse. The tibial nerve had been transected and repaired with a graft from a WT animal two weeks earlier. The approximate site of this repair is indicated by the white line and arrow. Above the repair site (in the proximal stump), there are more YFP+ axons, as indicated by increased fluorescence. The shorter axon profiles regenerating into the graft near the repair site are fairly irregular. Toward the bottom of the distal stump, longer regenerating sensory axons follow the regular pattern noted in the proximal stump.

Results and Discussion

Of the eight mice on which I performed a tibial nerve transection with a WT graft repair, it appears that three were improperly genotyped, as no fluorescence was found in either the proximal or the distal nerve stump. The nerves of a fourth mouse were damaged during mounting on slides and could not be imaged. In three mice the grafts had separated from the cut nerve so that they could not be studied. This unfortunate accumulation of experimental error left me with one exercised female mouse in which I could image the whole nerve transection and graft repair. Of the two nerves harvested from this animal, one had an improperly placed graft. In the remaining nerve, pictured above (Fig 3.1) excellent regeneration of both short and long axons into the WT graft was noted. All comparisons made to untreated and exercised WT animals (Fig 3.2) are from analysis of this nerve.

Despite the fact that I was only left with one nerve to analyze, some interesting findings emerged from analysis of measured axon profile lengths (Fig 3.2). The distribution of sensory axon profile lengths measured in this Advillin-Cre::YFP[f] mouse was compared to that from untreated and exercised female Thy-1-YFP-H mice reported previously (Wood et al., 2012). Only sensory axons are fluorescent in the Adv-Cre::YFP[f] mouse but both motor and sensory axons are fluorescent in the Thy-1-YFP-H strain.

Among regenerating axon profiles shorter than 1000 μm, similar proportions were found in the exercised Adv-Cre::YFP[f] mouse (sensory axons) and untreated Thy-1-YFP-H mice (both sensory and motor axons). Both of these distributions lie to the left of that of the lengths of profiles of regenerating axons in Thy-1-YFP-H mice that were exercised following nerve transection and repair. Thus, a greater proportion of regenerating axons had elongated only 1 mm or less during the two week survival period in either untreated Thy-1-YFP-H mice or the exercised Adv-Cre::YFP[f] mouse than in the exercised Thy-1-YFP-H mice. However, for longer axon profile lengths, especially between 1000 and
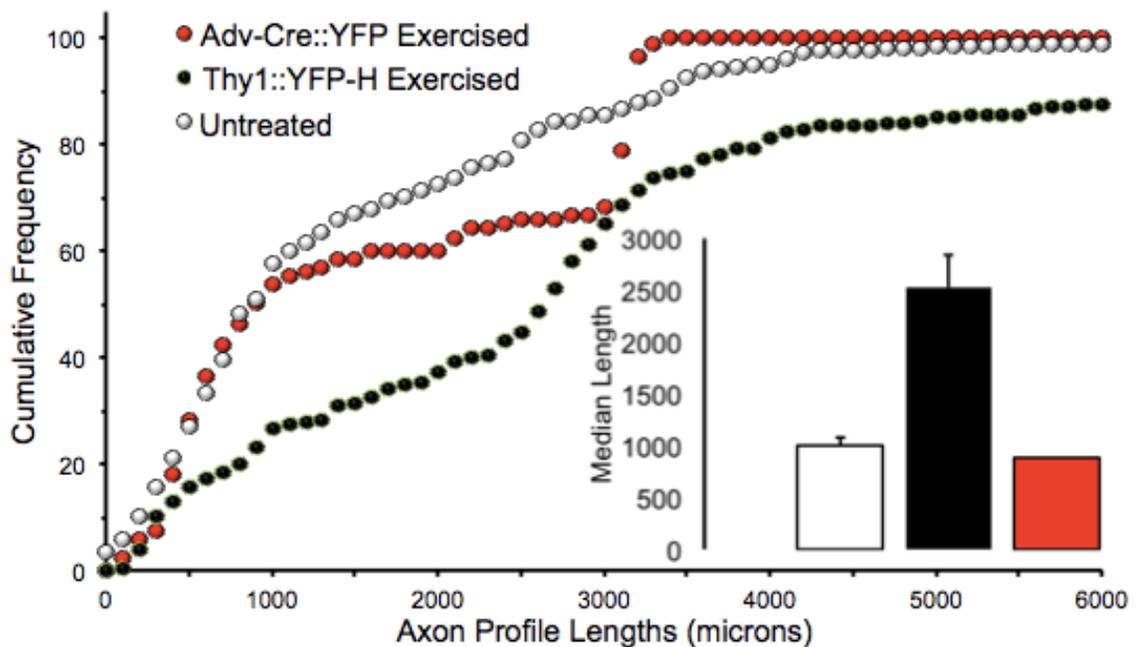
3000 μm, the distribution in the exercised Adv-Cre::YFP[f] mouse diverges from that of the untreated Thy-1-YFP-H mice. Within this same range of axon profile lengths, the distribution of sensory axon profile lengths in the Adv-Cre::YFP[f] mouse is also different from that of sensory and motor axon profile lengths in exercised Thy-1-YFP-H mice. Thus, exercise results in enhances sensory axon regeneratio in exercised Adv-Cre::YFP[f] mice, but this enhancement is less than that observed in exercised Thy-1-YFP-H mice, where both sensory and motor axons were studied. Even though it is impossible to differentiate between sensory and motor axon regeneration in Thy-1-YFP-H mice, one implication of these findings might be that exercise enhances motor axon regeneration to a greater extent than sensory axon regeneration.

A second measure of the extent of axon regeneration, median axon profile lengths is shown for the same three groups in the inset of Fig 3.2. The median from the one Adv-Cre::ChR2[f] mouse studied lies within the range noted for untreated Thy-1-YFP-H mice but considerably smaller than that noted in exercised Thy-1-YFP-H mice.

These findings are consistent with an interpretation that the regeneration of some, but not all of the YFP+ sensory axons in the Adv-Cre::ChR2[f] mouse is enhanced by exercise. This observation follows more recent optogenetics work in the English lab, but mechanism by which this enhancement occurs is not yet clear. Optical stimulation of cut and repaired nerves in the Adv-Cre::ChR2[f] mouse results in successful axon regeneration of more sensory neurons than untreated controls (Ward and English, 2015), suggesting that these neurons respond to increased activity in a manner similar to motoneurons. However, whether the activity of axotomized sensory neurons is increased during exercise remains unknown. In cats, nerve recordings were used to argue that the activity of sensory neurons during locomotion was nearly eliminated following peripheral injury and disconnection of the axons from their peripheral targets (Gordon et al., 1980). In recordings made from regenerating axons in treadmill walking

rats in the English lab (Gore et al., 2015; Srinivasan et al., 2016), single units with

phase-modulated continuous activity patterns, reminiscent of sensory axon discharge,

were encountered frequently. It is also possible that factors other than activity could

explain any enhancement of sensory axon regeneration with exercise. Repeating the

experimental results reported here will be an important first step in formulating testable

hypotheses.

Figure 3.2. A cumulative frequency histogram of axon profile lengths in an Advillin-Cre::YFP^f mouse vs. Thy-1-YFP-H mice following treadmill training.

The distribution of fluorescent regenerating axon profile lengths in three groups of mice is displayed as an overlaid cumulative frequency histograms. Data from an Adv-Cre::YFP^f animal (expresses YFP only in sensory axons) in which the tibial nerve was transected and repaired and then exercised for two weeks (red symbols) are compared to published data from Thy1::YFP-H animals (express YFP in both motor and sensory axons) which were similarly transected and repaired and either exercised (black symbols) or untreated (white symbols). Inset: average (±SEM) median axon profile lengths for three groups of animals.

References

Armbruster, B.N., Li, X., Pausch, M.H., Herlitze, S., and Roth, B.L. (2007). Evolving the lock to fit the key to create a family of G protein-coupled receptors potently activated by an inert ligand. Proceedings of the National Academy of Sciences of the United States of America *104*, 5163-5168.

Benkhelifa-Ziyyat, S., Besse, A., Roda, M., Duque, S., Astord, S., Carcenac, R., Marais, T., and Barkats, M. (2013). Intramuscular scAAV9-SMN injection mediates widespread gene delivery to the spinal cord and decreases disease severity in SMA mice. Molecular therapy : the journal of the American Society of Gene Therapy *21*, 282-290.

Duque, S., Joussemet, B., Riviere, C., Marais, T., Dubreil, L., Douar, A.M., Fyfe, J., Moullier, P., Colle, M.A., and Barkats, M. (2009). Intravenous administration of self-complementary AAV9 enables transgene delivery to adult motor neurons. Molecular therapy : the journal of the American Society of Gene Therapy *17*, 1187-1196.

English, A.W. (2005). Enhancing axon regeneration in peripheral nerves also increases functionally inappropriate reinnervation of targets. The Journal of Comparative Neurology *490*, 427-441.

English, A.W., Chen, Y., Carp, J.S., Wolpaw, J.R., and Chen, X.Y. (2007). Recovery of electromyographic activity after transection and surgical repair of the rat sciatic nerve. Journal of Neurophysiology *97*, 1127-1134.

English, A.W., Wilhelm, J.C., and Ward, P.J. (2014). Exercise, neurotrophins, and axon regeneration in the PNS. Physiology *29*, 437-445.

Farrell, M.S., and Roth, B.L. (2013). Pharmacosynthetics: Reimagining the pharmacogenetic approach. Brain Research *1511*, 6-20.

Federici, T., Taub, J.S., Baum, G.R., Gray, S.J., Grieger, J.C., Matthews, K.A., Handy, C.R., Passini, M.A., Samulski, R.J., and Boulis, N.M. (2012). Robust spinal motor neuron transduction following intrathecal delivery of AAV9 in pigs. Gene therapy *19*, 852-859.

Fortun, J., Puzis, R., Pearse, D.D., Gage, F.H., and Bunge, M.B. (2009). Muscle injection of AAV-NT3 promotes anatomical reorganization of CST axons and improves behavioral outcome following SCI. Journal of Neurotrauma *26*, 941-953.

Foust, K.D., Nurre, E., Montgomery, C.L., Hernandez, A., Chan, C.M., and Kaspar, B.K. (2009). Intravascular AAV9 preferentially targets neonatal neurons and adult astrocytes. Nature Biotechnology *27*, 59-65.

Gomez-Pinilla, F., Ying, Z., Opazo, P., Roy, R.R., and Edgerton, V.R. (2001). Differential regulation by exercise of BDNF and NT-3 in rat spinal cord and skeletal muscle. The European Journal of Neuroscience *13*, 1078-1084.

Gordon, T., Chan, K.M., Sulaiman, O.A., Udina, E., Amirjani, N., and Brushart, T.M. (2009). Accelerating axon growth to overcome limitations in functional recovery after peripheral nerve injury. Neurosurgery *65*, A132-144.

Gordon, T., Hoffer, J.A., Jhamandas, J., and Stein, R.B., Long-term effects of axotomy on neural activity during cat locomotion. (1980). Journal of Physiology (London) *303*, 243-63.

Gore, R.K., Choi, Y., Bellamkonda, R., and English, A. (2015). Functional recordings from awake, behaving rodents through a microchannel based regenerative neural interface. Journal of Neural Engineering,*12,* 016017*.*

Groves, M.L., McKeon, R., Werner, E., Nagarsheth, M., Meador, W., and English, A.W. (2005). Axon regeneration in peripheral nerves is enhanced by proteoglycan degradation. Experimental Neurology *195*, 278-292.

Hirakawa, M., McCabe, J.T., and Kawata, M. (1992). Time-related changes in the labeling pattern of motor and sensory neurons innervating the gastrocnemius muscle, as revealed by the retrograde transport of the cholera toxin B subunit. Cell and Tissue Research *267*, 419-427.

Jaiswal, P.A., and English, A. W. (2015). Pharmacogenetic enhancement of functional recovery from sciatic nerve transection. Abstr Soc Neurosci *517.04*.

Kaspar, B.K., Llado, J., Sherkat, N., Rothstein, J.D., and Gage, F.H. (2003). Retrograde viral delivery of IGF-1 prolongs survival in a mouse ALS model. Science (New York, NY) *301*, 839-842.

Kugler, S., Kilic, E., and Bahr, M. (2003). Human synapsin 1 gene promoter confers highly neuron-specific long-term transgene expression from an adenoviral vector in the adult rat brain depending on the transduced area. Gene Therapy *10*, 337-347.

Liske, H., Towne, C., Anikeeva, P., Zhao, S., Feng, G., Deisseroth, K., and Delp, S. (2013). Optical inhibition of motor nerve and muscle activity in vivo. Muscle & Nerve *47*, 916-921.

MacGillivray, T.E. (2003). Fibrin sealants and glues. Journal of Cardiac Surgery *18*, 480-485.

Nichols, C.D., and Roth, B.L. (2009). Engineered G-protein Coupled Receptors are Powerful Tools to Investigate Biological Processes and Behaviors. Frontiers in Molecular Neuroscience *2*, 16.

Noble, J., Munro, C.A., Prasad, V.S., and Midha, R. (1998). Analysis of upper and lower extremity peripheral nerve injuries in a population of patients with multiple injuries. The Journal of Trauma *45*, 116-122.

Price, J. (1985). An immunohistologicaland quantitative examine of dorsal root ganglion subpopulations. The Journal of Neuroscience *5*, 2051-2069.

Rahim, A.A., Wong, A.M., Hoefer, K., Buckley, S.M., Mattar, C.N., Cheng, S.H., Chan, J.K., Cooper, J.D., and Waddington, S.N. (2011). Intravenous administration of AAV2/9 to the fetal and neonatal mouse leads to differential targeting of CNS cell types and extensive transduction of the nervous system. FASEB Journal *25*, 3505-3518.

Sabatier, M.J., Redmon, N., Schwartz, G., and English, A.W. (2008). Treadmill training promotes axon regeneration in injured peripheral nerves. Experimental Neurology *211*, 489-493.

Samaranch, L., Salegio, E.A., San Sebastian, W., Kells, A.P., Bringas, J.R., Forsayeth, J., and Bankiewicz, K.S. (2013). Strong cortical and spinal cord transduction after AAV7 and AAV9 delivery into the cerebrospinal fluid of nonhuman primates. Human Gene Therapy *24*, 526-532.

Srinivasan, A., Tipton, J., Tahilramani, M., Kharbouch, A., Gaupp, E., Song, C., Venkataraman, P., Falcone, J., Lacour, S.P., Stanley, G.B., English, A.W., and Bellamkonda, R.V. (2016). A regenerative microchannel device for recording multiple single-unit action potentials in awake, ambulatory animals. The European Journal of Neuroscience *43*, 474-85.

Scholz, T., Krichevsky, A., Sumarto, A., Jaffurs, D., Wirth, G.A., Paydar, K., and Evans, G.R. (2009). Peripheral nerve injuries: an international survey of current treatments and future perspectives. Journal of reconstructive microsurgery *25*, 339-344.

van den Pol, A.N., and Ghosh, P.K. (1998). Selective neuronal expression of green fluorescent protein with cytomegalovirus promoter reveals entire neuronal arbor in transgenic mice. The Journal of Neuroscience *18*, 10640-10651.

Ward, P.J., Jones, L.N., Mulligan, A., Goolsby, W., Wilhelm, J.C., and English, A.W. (2016). Optically-induced Neuronal Activity is Sufficient to Promote Functional Motor Axon Regeneration In Vivo. PLoS One *IN PRESS*.

Ward, P.J, and English, A.W. (2015). Large-diameter sensory neurons require androgen receptor signaling for activity-enhanced axon regeneration. Abstr Soc Neurosci *517.06*.

Wilhelm, J.C., Xu, M., Cucoranu, D., Chmielewski, S., Holmes, T., Lau, K.S., Bassell, G.J., and English, A.W. (2012). Cooperative roles of BDNF expression in neurons and Schwann cells are modulated by exercise to facilitate nerve regeneration. The Journal of Neuroscience *32*, 5002-5009.

Wood, K., Wilhelm, J.C., Sabatier, M.J., and English, A.W. (2012). Sex differences in the effects of treadmill training on axon regeneration in cut peripheral nerves. Developmental Neurobiology *72*, 688-698.

Zurborg, S., Piszczek, A., Martinez, C., Hublitz, P., Al Banchaabouchi, M., Moreira, P., Perlas, E., and Heppenstall, P.A. (2011). Generation and characterization of an Advillin-Cre driver mouse line. Molecular Pain *7*, 66.